

because fiber dispersion curves (both Yb-doped and single mode) can vary significantly from manufacturing specifications and from fiber to fiber. Therefore, we first measured the cavity dispersion *in situ* using the technique of Knox [13]. By putting a slit that is narrower than the beam profile in front of the retroreflection mirror (M1 in Fig. 1), the optical spectrum, and thus the central wavelength of the mode-locked laser, can be scanned. The width of the mode-locked spectrum remains no less than 75% of the unfiltered spectrum. As the slit is scanned, the free-running repetition rate (f_{rep}) is monitored with a photodiode and recorded with a frequency counter. Differentiating the group delay, $T_g (= 1/f_{\text{rep}})$ versus the center frequency of the optical spectra (ω_0) yields the net-cavity GDD. The experimental results for four grating separations are shown in Fig. 2 (circles). The solid lines in Fig. 2 are the calculated dispersion based on the sum of the elements inside the cavity, including reasonable estimates of fiber dispersion (Yb fiber estimate from [14] and SMF from FLEX 1060 fiber data), dispersion from high-refractive-index materials (glass optics and terbium gallium garnet [15], a material found in optical isolators), and grating dispersion [16]. The results show that the four mode-locked spectra in the inset of Fig. 1 correspond to one anomalous, one near-zero, and two normal-dispersion regimes. While third-order dispersion is evident in the slope of the lines in Fig. 2, we define the net-cavity GDD (from normal to anomalous) using the second-order dispersion value at the nominal center wavelength (1035 nm for all spectra in Fig. 1).

With a clear understanding of the cavity dispersion, we measured the free-running offset frequency, f_{CEO} , of the laser operating in several dispersion modes. To this end, we first amplified the chirped oscillator output in a core-pumped Yb-doped fiber amplifier then recompressed the pulses with an external double-pass grating pair (average power ~ 400 mW, 80 fs pulse duration). Continuum generation was achieved with a 15 cm piece of nonlinear suspended-core fiber [17]. An f_{CEO} beat was then measured with a standard f - $2f$ interferometer [18]. The microwave spectra of two sample f_{CEO} beat signals are shown in Fig. 3(a) for the normal- and zero-dispersion regimes, illustrating the significant difference in linewidth. Similar effects have been observed in other Er and Yb laser systems [19]; however, to our knowledge, this dependence has not been mapped over a range of cavity dispersions.

A complete set of measurements of the free-running f_{CEO} linewidth versus dispersion is given in Fig. 3(b). A clear trend of decreasing f_{CEO} linewidth toward zero

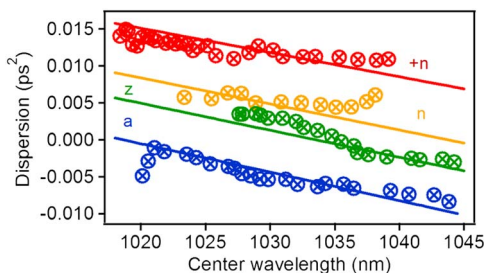


Fig. 2. (Color online) Experimental measurement of the laser cavity GDD (circles) and calculation of dispersion as a sum of all the cavity elements (solid lines).

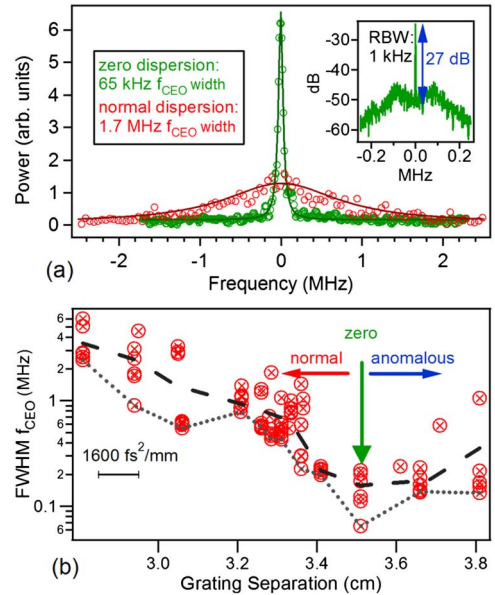


Fig. 3. (Color online) (a) Spectrum of free-running f_{CEO} beat at normal- and zero-dispersion points with Lorentzian fits. Inset, locked f_{CEO} beat. (b) Collection of f_{CEO} linewidths versus net-cavity dispersion (measured by grating separation): dotted curve, minimum linewidth obtained and dashed curve, average value.

dispersion (from both the normal and anomalous sides) is seen. For each dispersion regime (i.e., a fixed grating separation), the f_{CEO} linewidth can also change with pump power (which directly affects the internal cavity circulating power and the spectral width of the pulse). At each grating separation, the pump power was tuned within the full range of stable mode locking (i.e., no cw breakthrough). Many factors, including the pumping rate, cavity loss, and the laser's nonlinear response can impact the f_{CEO} linewidth, including the “turning points” [20] of the f_{CEO} beat and the polarization settings. Nevertheless, in the normal-dispersion mode, we never obtained an f_{CEO} linewidth as narrow as in the zero-dispersion regime.

As the microwave power spectrum [Fig. 3(a)] can ambiguously mix amplitude and frequency noise, we also directly measured the frequency noise spectrum of f_{CEO} . This was accomplished by sending the f_{CEO} beat signal into a frequency divider followed by a delay line discriminator and a vector signal analyzer. These results are given in Fig. 4(a) for laser operation at normal and zero dispersion, corresponding to measured free-running f_{CEO} widths of 1.45 MHz and 130 kHz, respectively. The broad f_{CEO} beat clearly has considerably higher FM noise. Calculation of rf spectra from the frequency noise spectra in Fig. 4(a) (using numerical methods) yields a FWHM of 1.50 MHz (normal) and 104 kHz (zero), a correspondingly 3% and 20% deviation from the experimental values. This might suggest a small contribution from AM noise in the zero-dispersion regime, while the much higher FM noise in the normal regime masks any AM contribution. Nonetheless, it is clear that the frequency noise dominates the f_{CEO} linewidths. It is also possible to tightly lock the f_{CEO} beat in the zero-dispersion regime, as shown in the inset of Fig. 3(a), where the coherent signature on a undivided copy of f_{CEO} (at 226 MHz) is seen.

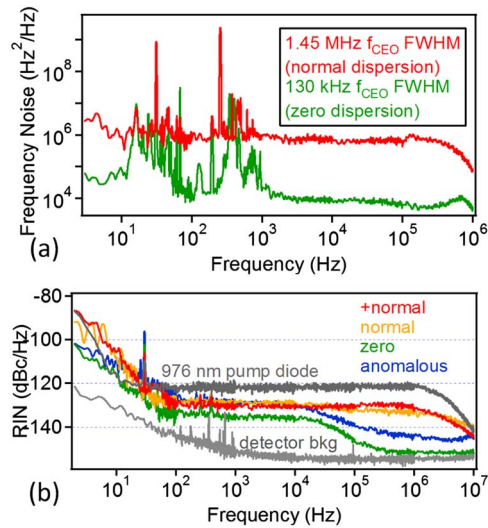


Fig. 4. (Color online) (a) Frequency noise on two sample f_{CEO} beat signals (division factor included to give true f_{CEO} noise). (b) Amplitude noise (RIN) for four dispersion regimes.

In this spectrum, 90% of the power is located within the coherent carrier.

In most frequency combs, there is a strong coupling between amplitude and frequency noise. The amplitude noise of the laser oscillator was measured [Fig. 4(b)] at the same four net-cavity-dispersion regimes shown in Figs. 1 and 2. Amplitude noise was measured by monitoring a portion of the laser output with a fast photodiode (1 GHz bandwidth) and using a vector signal analyzer to obtain a power spectral density of the relative intensity noise ($\text{RIN} = [\Delta P_{\text{rms}}/P_o]^2$ per Hz bandwidth, where P is the optical power). We observed significant differences in the RIN as a function of net-cavity dispersion, with zero net-cavity dispersion having the lowest RIN. It is not possible to state that “all other parameters are equal” except the dispersion when comparing the different laser operating modes. Each dispersion point requires adjustment of the pump diode power and waveplate settings in order to achieve stable mode locking, leading to differences in output coupling and cavity Q . However, in practice, the zero-dispersion mode consistently shows the lowest RIN. We also present the pump laser RIN in Fig. 4(b). The white-noise level of the pump RIN is nearly constant with the changing pump current (data not shown), and it is on average 10 dB higher than the oscillator RIN.

Experimentally, the Yb-fiber oscillator presented here operates in its quietest mode near zero dispersion, including reduced amplitude noise on the oscillator, narrowest f_{CEO} linewidth, and less frequency noise on f_{CEO} itself. This fact alone should be important for the further development of such lasers for frequency comb applications. Additionally, it is interesting to note that our measurements of f_{CEO} noise are consistent with the prediction of minimum timing jitter for stretched-pulse fiber lasers near zero net-cavity dispersion [9,21]. This could imply a direct correlation between noise on f_{CEO} and f_{rep} , where ASE-induced center wavelength changes are coupled to timing jitter through the group velocity dispersion [9,10,21]. However, the connection between various noise sources and the frequency noise

on the comb itself can be complicated [9,12,21,22], and direct measurements of the timing jitter would help provide a more complete picture of the noise properties of Yb-fiber laser combs [23].

The authors thank IMRA America, Inc., for the use of the suspended-core nonlinear fiber [17]. This research was funded in part by the United States Department of Homeland Security’s Science and Technology Directorate through the National Institute of Standards and Technology (NIST). We further thank Ingmar Hartl, Nate Newbury, Frank Quinlan, and Alex Zolot for helpful comments. Any mention of commercial products does not constitute an endorsement by NIST.

References

1. X. Zhou, F. Yoshitomi, Y. Kobayashi, and K. Torizuka, *Opt. Express* **16**, 7055 (2008).
2. T. Schibli, I. Hartl, D. Yost, M. Martin, A. Marcinkevicius, M. Fermann, and J. Ye, *Nat. Photon.* **2**, 355 (2008).
3. M. Fermann and I. Hartl, *IEEE J. Sel. Top. Quantum Electron.* **15**, 191 (2009).
4. I. Hartl, L. Fu, B. Thomas, L. Dong, M. Fermann, J. Kim, F. Kartner, and C. Menyuk, in *Conference on Lasers and Electro-Optics/Quantum Electronics and Laser Science Conference and Photonic Applications Systems Technologies*, OSA Technical Digest (CD) (Optical Society of America, 2008), paper CTuC4.
5. F. Adler, K. Cossel, M. Thorpe, I. Hartl, M. Fermann, and J. Ye, *Opt. Lett.* **34**, 1330 (2009).
6. T. Johnson and S. Diddams, in *Conference on Lasers and Electro-Optics*, OSA Technical Digest (CD) (Optical Society of America, 2010), paper CPDB11.
7. D. Yost, T. Schibli, J. Ye, J. Tate, J. Hostetter, M. Gaarde, and K. Schafer, *Nat. Phys.* **5**, 815 (2009).
8. F. Wise, A. Chong, and W. Renninger, *Laser Photon. Rev.* **2**, 58 (2008).
9. N. Newbury and B. Swann, *J. Opt. Soc. Am. B* **24**, 1756 (2007).
10. J. Gordon and H. Haus, *Opt. Lett.* **11**, 665 (1986).
11. O. Prochnow, R. Paschotta, E. Benkler, U. Morgner, J. Neumann, D. Wandt, and D. Kracht, *Opt. Express* **17**, 15525 (2009).
12. B. Washburn and N. Newbury, *IEEE J. Quantum Electron.* **41**, 1388 (2005).
13. W. H. Knox, *Opt. Lett.* **17**, 514 (1992).
14. L. Grüner-Nielsen, S. Ramachandran, K. Jesperen, S. Ghalmi, M. Garmund, and B. Palsdottir, *Proc. SPIE* **6873**, 68730Q (2008).
15. U. Sugg and B. Schlarb, *Phys. Status Solidi (b)* **182**, K91 (1994).
16. A. M. Weiner, *Ultrafast Optics* (Wiley, 2009).
17. L. Dong, B. K. Thomas, and L. Fu, *Opt. Express* **16**, 16423 (2008).
18. D. Jones, S. Diddams, J. Ranka, A. Stentz, R. Windeler, J. Hall, and S. Cundiff, *Science* **288**, 635 (2000).
19. N. Kuse and Y. Kobayashi, The University of Tokyo Institute for Solid State Physics, Kashiwanoha 5-1-5, Kashiwa, Chiba 277-8581, Japan; I. Hartl, IMRA America, 1044 Woodridge Avenue, Ann Arbor, Michigan 48105, USA (personal communication, 2010).
20. K. Holman, R. Jones, A. Marian, S. Cundiff, and J. Ye, *Opt. Lett.* **28**, 851 (2003).
21. S. Namiki and H. Haus, *IEEE J. Quantum Electron.* **33**, 649 (1997).
22. H. Telle, B. Liphardt, and J. Stenger, *Appl. Phys. B* **74**, 1 (2002).
23. Y. Song, K. Jung, and J. Kim, arXiv:1102.1046v1 (2011).